Electronic Supplementary Material (ESI) for ChemComm.

Electronic Supplementary Information

Boosting oxygen reduction activity with low-temperature derived high-loading atomic cobalt on nitrogen-doped graphene for efficient Zn-air batteries

1. Experimental section

Material synthesis

Graphene oxide (GO) was beforehand prepared by a modified Hummers method. To prepare CoNG, 5 mL of 6×10^{-3} M cobalt acetate solution was added into 5 mL of graphene oxide aqueous solution (2 mg/mL) under magnetic stirring at room temperature. The mixed solution was lyophilized for 72 h and finally annealed in flowing NH_3 at different temperatures from 300 ˚C to 400 ˚C for 2 h with the heating rate of 2 ˚C/min. Controlled samples with different Co loading on nitrogen-doped graphene were also synthesized through the same procedures, except that the concentration of cobalt acetate was changed to be 0, 3×10^{-3} and 18×10^{-3} M for NG, $Co_{0.5}$NG and Co_3NG, respectively.

Characterizations

Scanning electron microscopy (SEM) images were observed with a JEOL-7100F. transmission electron microscopy (TEM) images were collected on a Titan G2 60-300 with image corrector and energy-dispersive X-ray (EDX) spectra were recorded using an Oxford IE250 system. Raman spectra were obtained using a Renishaw INVIA micro-Raman spectroscopy system. X-ray photoelectron spectroscopy (XPS) and ultraviolet photoelectron spectroscopy (UPS) measurements were conducted using an ESCALAB 250Xi instrument. Elemental content was analyzed using a Vario EL cube for CHNS/O analysis and PerkinElmer Optima 4300DV spectrometer for inductively coupled plasma optical emission spectrometry (ICP-OES) test. The X-ray adsorbed spectra (XAS) measured at Co K-edge was performed at the Advanced Photon Source (APS) of Argonne National Laboratory on the bending-magnet beamline 9-BM-B with electron energy of 7 GeV and average current of 100 mA. The radiation was monochromatized by a Si (111) double-crystal monochromator. Harmonic rejection was accomplished with Harmonic rejection mirror. All spectra were collected in transmission mode. XAS data reduction and analysis were processed by Athena software.

Electrochemical measurements

Electrocatalytic performance of ORR was measured on a CHI 760D electrochemical workstation linked with a RDE/RRDE instrument (PINE Co., Ltd.), and all the tests were carried out in O_2 saturated 0.1 M KOH aqueous solution using a three electrode system. A saturated calomel electrode (SCE) and a graphitic rod were used as the counter and reference electrodes, respectively. A glassy carbon (GC) disk electrode of RDE (diameter = 5.0 mm) loaded with catalyst ink was used as the working electrode: the catalyst ink was prepared by mixing 5 mg of catalyst powder and 5 mg of Vulcan XC-72R (VXC-72R) into 1 mL of solution consisting of 800 μL of isopropanol, 150 μL of deionized water and 50 μL of 5 wt% Nafion followed with fully ultrasonic dispersion; 10 μL of catalyst ink was dropped on the disk electrode, and then dried at room temperature before use.

CV and LSV curves were scanned in the potential range of 0.1 ~ 0.8 V (vs. SCE) at 5 mV s^{-1}, and the rotation rate for LSV tests were controlled at 400, 625, 900, 1225 and 1600 rpm, respectively. To further analyze the electron transfer numbers (n) and the peroxide yields, 12.5 uL of the catalyst ink was dropped on the glassy carbon disk electrode (diameter = 5.6 mm) of RRDE, and LSV tests were also carried out with the rotation rate kept at 1600 rpm and the potential of Pt ring electrode

set at 0.5 V (vs. SCE).

All the potentials measured above were converted to the scale of reversible hydrogen electrode (RHE) with the following Nernst equation: $E_{RHE} = E_{SCE} + (0.242 + 0.0593 \times pH)$.

The electron transfer number was calculated from Koutecky−Levich equation:

$$\frac{1}{j} = \frac{1}{j_L} + \frac{1}{j_K} = \frac{1}{0.62nFC_0(D_0)^{2/3}v^{-1/6}\omega^{1/2}} + \frac{1}{nFkC_0}$$

where j, j_L and j_K are the measured, diffusion-limiting and kinetic current densities, respectively; n is the electron transfer number; F is the faraday constant; C_0 is the saturated concentration of O_2 in 0.1 M KOH; D_0 is the diffusion coefficient of O_2; v is the kinetic viscosity of solution and ω is the rotation rate of the electrode.

The peroxide yields (HO_2^- %) and electron transfer number (n) can be calculated as the following equations:

$$n = 4\frac{I_d}{I_d + I_r / N} \qquad \mathrm{HO_2^-} = 200\frac{I_r / N}{I_d + I_r / N}$$

where I_r is the ring current, I_d is the disk current, and N is the collection efficiency of Pt ring electrode of RRDE (0.37).

Electrochemical performance on primary Zn-air batteries was also assessed. Primary Zn-air batteries were assembled with hydrophobic carbon fiber paper loaded with catalyst ink as the air cathode (catalyst ink was prepared as described in ORR test; active material loading is 1 mg cm^{-2}; the cathode area is 1 x 1 cm^2), metallic zinc plate as the anode (Zn is kept enough and excess without the risk of Zn derived battery decay), and the electrochemical performance was measured in 6 M KOH using a customized electrochemical cell. Pure O_2 was kept flowing into the air cathode throughout the measurements unless otherwise noted. The polarization curves were collected by LSV with a scan rate of 10 mV s^{-1} and the durability was tested at constant current density of 10 mA cm^{-2}. The electrochemical data was iR corrected (R = 1.25 Ω).

To assess the specific discharge capacity and energy density, Zn plate with the diameter of 1 cm and the thickness of 0.25 cm was used, while all the other details are kept. The data was presented without iR correction.

2. Supplemental figures and tables

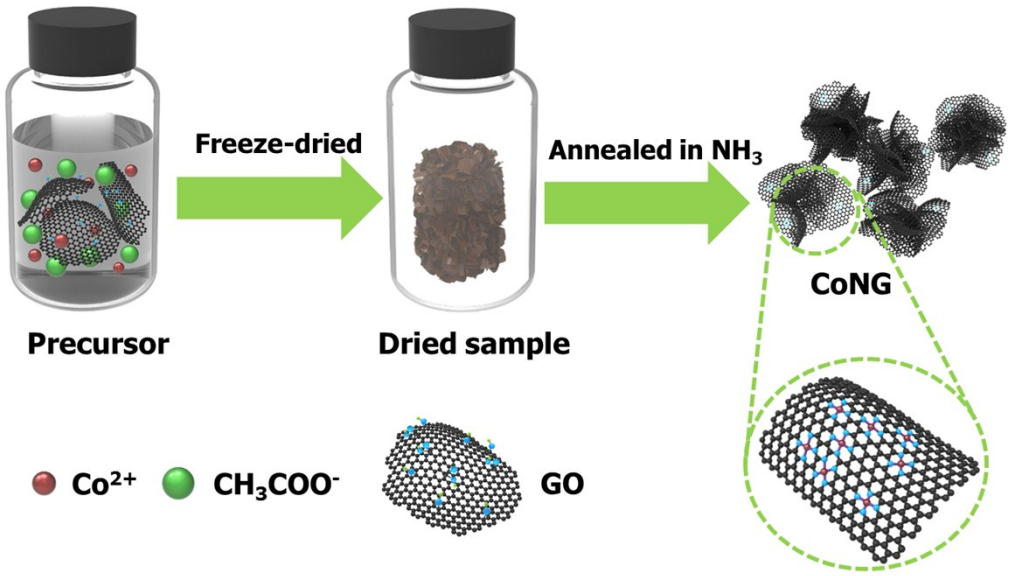

Fig. S1 Scheme for the synthesis of CoNG. The main formation mechanism is described as follows. The rich oxygen functional groups in the as-prepared GO can first ensure strong interaction with Co^{2+} ions in the solution, and the Co^{2+} ions will mainly locate in the defects of GO after freeze-dry treatment; the low-temperature treatment in NH_3 condition can then induce the reduction of GO, the doping of nitrogen, and the incorporation of metal atoms into graphene lattices.

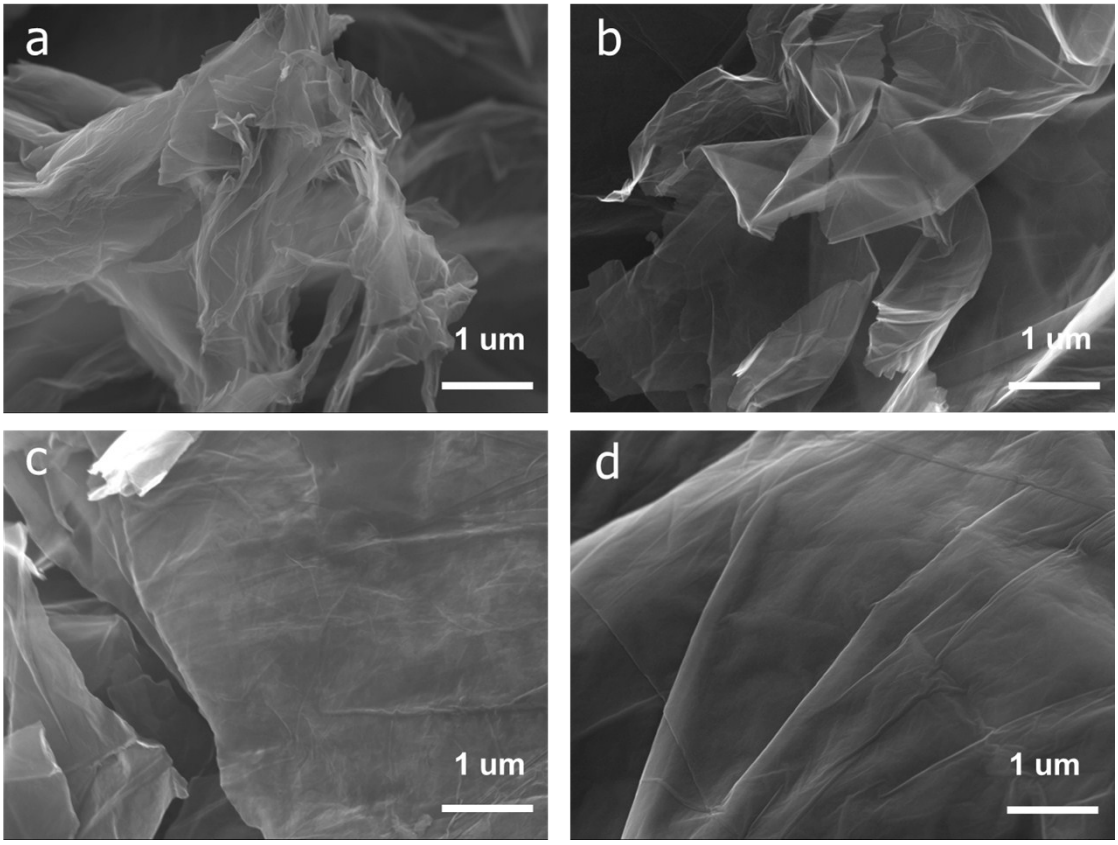

Fig. S2 SEM images of (a) NG-350, (b) CoNG-300, (c) CoNG-350 and (d) CoNG-400.

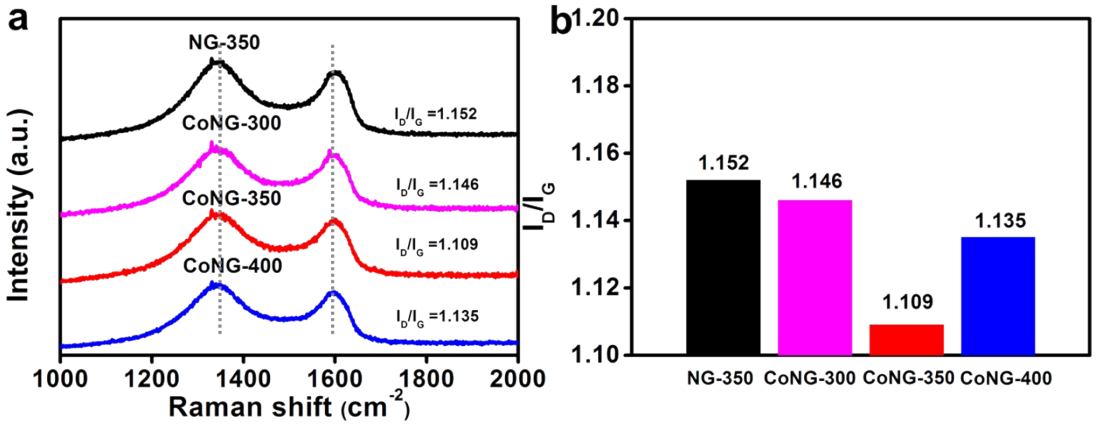

Fig. S3 (a) Raman spectra of CoNG-300, CoNG-350, CoNG-400, NG-350, and (b) the corresponding values of I_D/I_G.

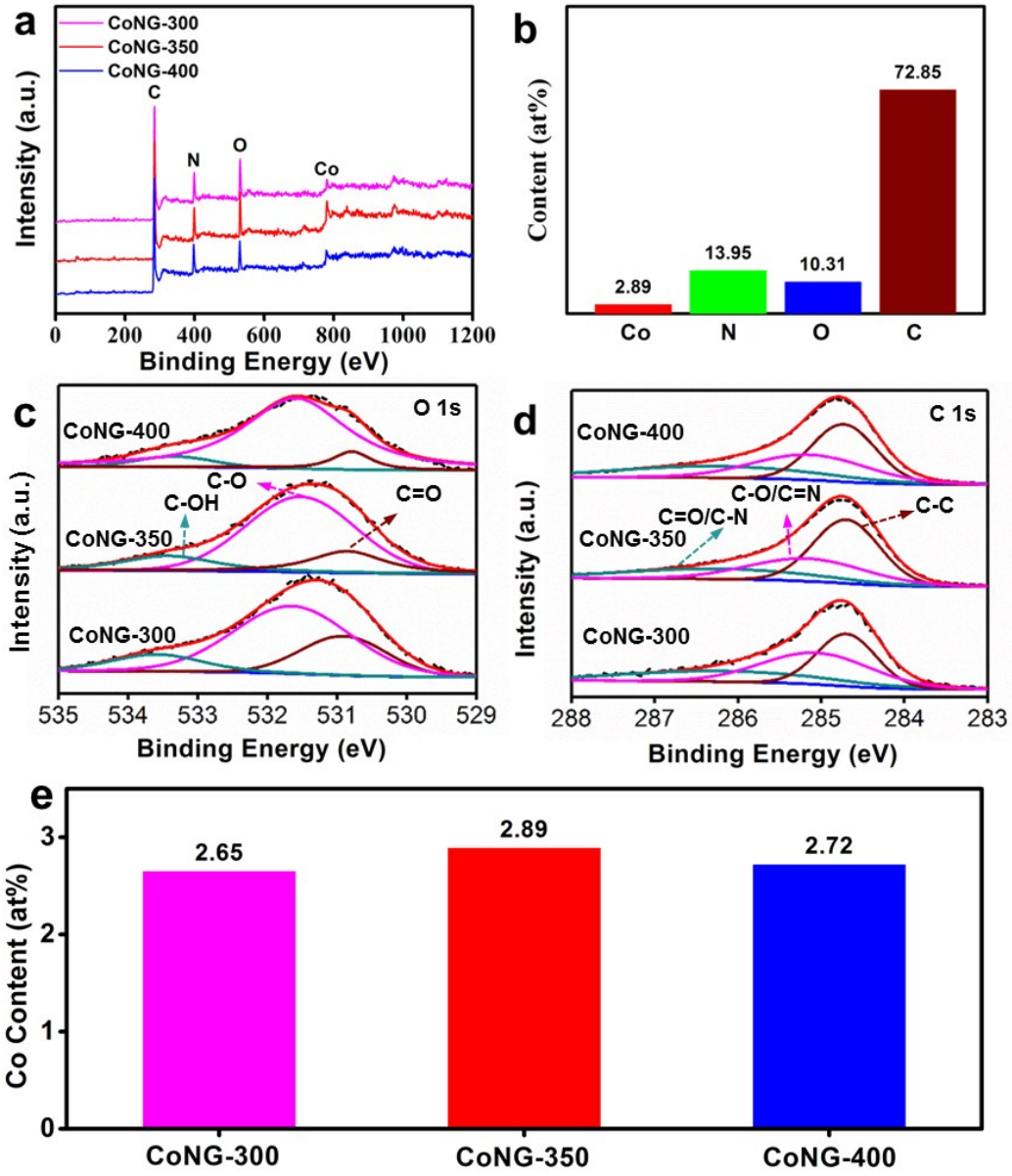

Fig. S4 (a) XPS survey spectra, (c) O 1s core-level and (d) C 1s core-level XPS spectra of CoNG-300, CoNG-350 and CoNG-400; (b) elemental percentages of cobalt, nitrogen, oxygen and carbon in CoNG-350 measured by ICP-OES and CHNO elemental analyzer; (e) Co content of CoNG-300, CoNG-350 and CoNG-400 measured by ICP-OES.

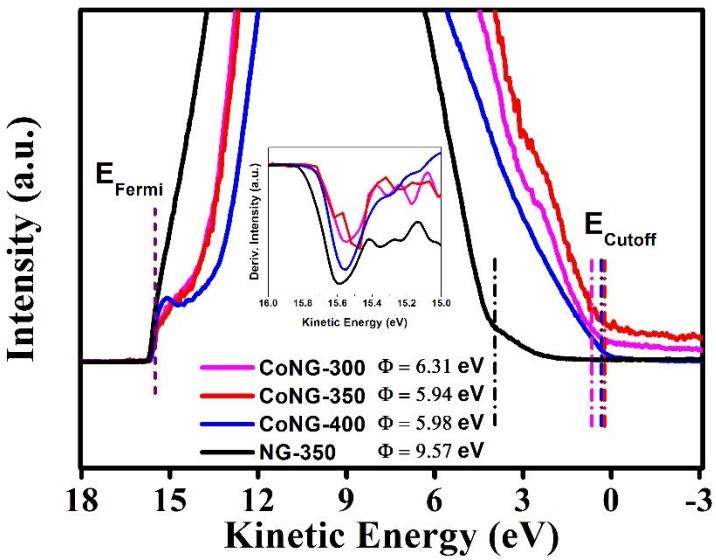

Fig. S5 UPS spectra collected using He I (21.21 eV) radiation. The inelastic cutoff (E_{cutoff}) and Fermi edge (E_{Fermi}) are shown with dash lines. The inset shows the derivative intensity vs kinetic energy, and the strong peaks present the Fermi edge. The work function (ϕ) is calculated as follows: $\phi = 21.21 - (E_{Fermi} - E_{cutoff})$ eV

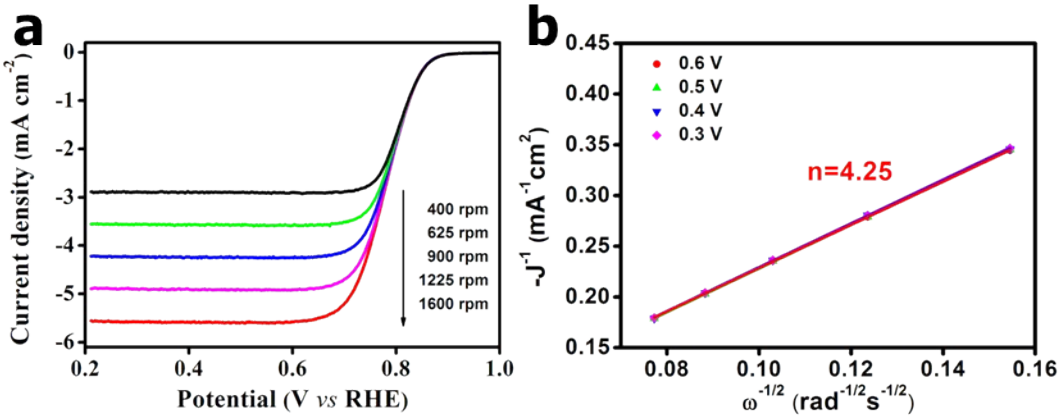

Fig. S6 (a) ORR polarization curves of CoNG-350 at various rotation rates, (b) Koutecky-Levich plots of CoNG-350 obtained at different potentials.

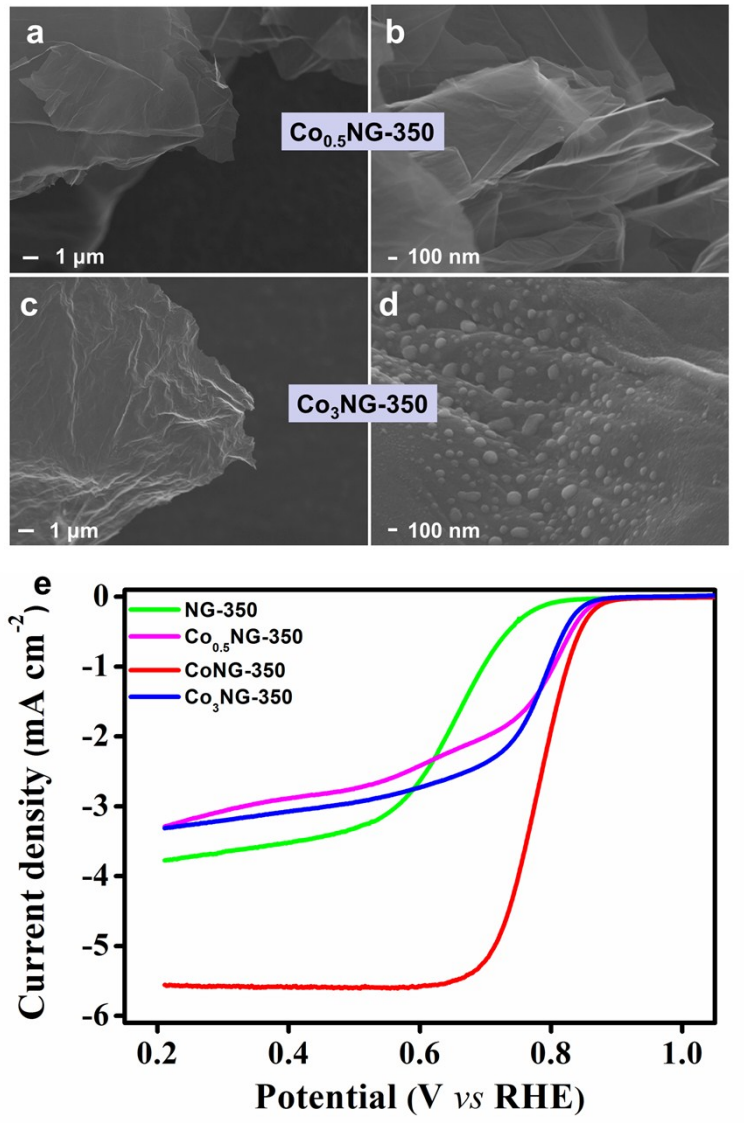

Fig. S7 SEM images of (a-b) $Co_{0.5}$NG-350 and (c-d) Co_3NG-350. (e) ORR performance comparisons of "CoNG" with different Co content, and the polarization curves were obtained in O_2-saturated 0.1 M KOH solution with rotation speed at 1600 rpm.

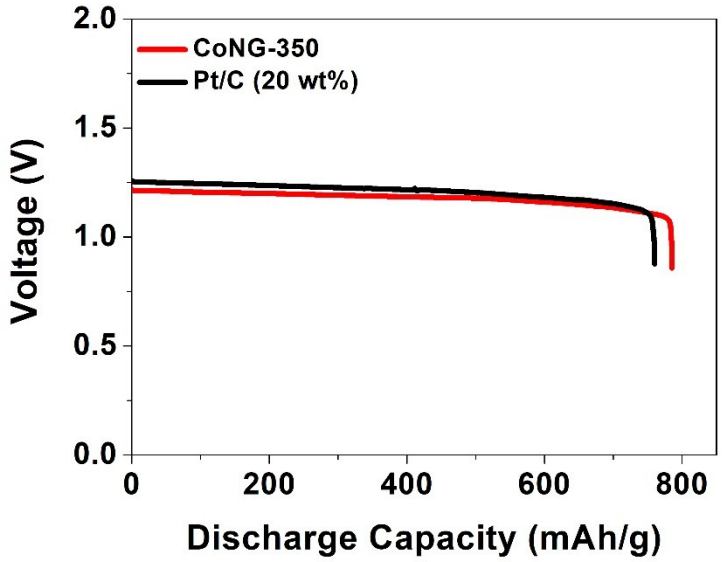

Fig. S8 Discharge curves (without iR corrected) of CoNG-350 and Pt/C based primary Zn-air batteries at the current density of 10 mA cm^{-2}. It should be pointed out that Zn plate with the diameter of 1 cm and the thickness of 0.25 cm was used as the anode.

The specific discharge capacity and energy density are normalized to the mass of Zn plate. The specific discharge capacity of CoNG-350 and Pt/C is 785 and 760 mAh g^{-1}, respectively. The energy density of CoNG-350 is calculated to be 926 Wh kg^{-1}, almost the same with that of Pt/C (927 Wh kg^{-1}).

Table S1. Comparisons of synthesis temperature and atom/mass loading of different transition metal-based single-atom catalysts, and the limiting diffusion current density is also compared.

Catalysts	Synthesis Temperature (℃)	Atom/Mass Loading	Limiting Diffusion Current Density (mA cm^{-2})	References
CoNG-350	**350**	**2.89 at% 12.85 wt%**	**[a]5.60**	**This work**
Co-MOF-C_2-900	900	1.20 at% 5.58 wt%	**[a]5.50**	***Adv Mater*** 2018, 30, 1705431
Co-Nx-C	950	1.23 wt% 5.77 wt%	**[a]4.75**	***Adv Mater*** 2017, 29, 1703185
Co@NG	700	/	**[b]4.00**	***Adv Funct Mater*** 2016, 26, 4234
Co-N/CNT	900	/	**[a]4.00**	***Adv Funct Mater*** 2017, 27, 1606034
$CoO_{0.83}S_{0.17}$/GN	700	/	**[a]4.12**	***Adv Mater*** 2017,29, 1702526
Co-N-C HHMTS-24	800	0.25 at% 1.17 wt%	**[a]5.50**	***small*** 2017, 13, 1603437
D-NC	1050	/	**[a]4.40**	***Chem Commun*** 2016, 52, 8156
Fe-N_4 Sac/NPC	920	0.42 at% 1.96 wt%	**[a]4.90**	***Angew Chem Int Ed*** 2018, 57, 8614
S,N-Fe/N/C-CNT	700	0.70 at% 3.28 wt%	**[a]5.70**	***Chem Sci*** 2016, 7, 5758

Note: a and b suggest that the electrolyte are 0.1 KOH and 1.0 KOH, respectively.